AUTHOR(S):

Kojima, Kotaro; Takewaki, Izuru

frontiers
in Built Environment

Critical earthquake response of elastic–plastic structures under near-fault ground motions (Part 1: Fling-step input)

Kotaro Kojima and Izuru Takewaki*

Department of Architecture and Architectural Engineering, Graduate School of Engineering, Kyoto University, Kyoto, Japan

The double impulse input is introduced as a substitute of the fling-step near-fault ground motion and a closed-form solution of the elastic–plastic response of a structure by the "critical double impulse input" is derived. Since only the free-vibration appears under such double impulse input, the energy approach plays an important role in the derivation of the closed-form solution of a complicated elastic–plastic response. It is shown that the maximum inelastic deformation can occur either after the first impulse or after the second impulse depending on the input level. The validity and accuracy of the proposed theory are investigated through the comparison with the response analysis to the corresponding one-cycle sinusoidal input as a representative of the fling-step near-fault ground motion. Since the critical input means the resonant case, the present theory dealing with the resonant response should be applied to buildings except very flexible ones.

Introduction

The effects of near-fault ground motions on structural response have been investigated extensively (Bertero et al., 1978; Hall et al., 1995; Sasani and Bertero, 2000; Alavi and Krawinkler, 2004; Mavroeidis et al., 2004; Kalkan and Kunnath, 2006, 2007; Xu et al., 2007; Rupakhety and Sigbjörnsson, 2011; Yamamoto et al., 2011; Khaloo et al., 2015; Vafaei and Eskandari, 2015). The fling-step and forward-directivity are widely recognized as special keywords to characterize such near-fault ground motions (Mavroeidis and Papageorgiou, 2003; Bray and Rodriguez-Marek, 2004; Kalkan and Kunnath, 2006; Mukhopadhyay and Gupta, 2013a,b; Zhai et al., 2013; Hayden et al., 2014; Yang and Zhou, 2014). Especially, Northridge earthquake in 1994, Hyogoken-Nanbu (Kobe) earthquake in 1995, and Chi-Chi (Taiwan) earthquake in1999 raised special attention to many earthquake structural engineers.

The fling-step and forward-directivity inputs have been characterized by two or three wavelets. For this class of ground motions, many useful research works have been conducted. Mavroeidis and Papageorgiou (2003) investigated the characteristics of this class of ground motions in detail and proposed some simple models (for example, Gabor wavelet and Berlage wavelet). Xu et al. (2007) employed a kind of Berlage wavelet and applied it to the performance evaluation of passive energy dissipation systems. Takewaki and Tsujimoto (2011) used the Xu's approach and proposed a method for scaling ground motions from the viewpoints of drift and input energy demand. Takewaki et al. (2012) employed a sinusoidal wave for pulse-type waves. In this paper, a new approach based on the

京都大学
KYOTO UNIVERSITY

Kojima and Takewaki

KURENAI 紅
京都大学学術情報リポジトリ
Kyoto University Research Information Repository

Elastic–plastic near-fault response

double impulse (Kojima et al., 2015a) is proposed and the intrinsic response characteristics by the near-fault ground motion are captured.

Most of the previous works on the near-fault ground motions deal with the elastic response because the number of parameters (e.g., duration and amplitude of pulse, ratio of pulse frequency to structure natural frequency, change of equivalent natural frequency for the increased input level) to be considered on this topic is many and the computation itself of elastic–plastic response is quite complicated.

In order to tackle such important but complicated problem, the double impulse input is introduced as a substitute of the fling-step near-fault ground motion and a closed-form solution of the elastic–plastic response of a structure by the "critical double impulse input" is derived. It is shown that, since only the free-vibration appears under such double impulse input, the energy approach plays an important role in the derivation of the closed-form solution of a complicated elastic–plastic response. It is also shown that the maximum inelastic deformation can occur either after the first impulse or after the second impulse depending on the input level. The validity and accuracy of the proposed theory are investigated through the comparison with the response analysis result to the corresponding one-cycle sinusoidal input as a representative of the fling-step near-fault ground motion. The amplitude of the double impulse is modulated so that its maximum Fourier amplitude coincides with that of the corresponding one-cycle sinusoidal input.

The closed-form or nearly closed-form solutions of the elastic–plastic earthquake response have been obtained so far only for the steady-state response to sinusoidal input or the transient response to an extremely simple sinusoidal input (Caughey, 1960a,b; Roberts and Spanos, 1990; Liu, 2000). In this paper, the following motivation is raised. If a near-fault ground motion can be represented by a double impulse, the elastic–plastic response (continuation of free-vibrations) can be derived by an energy approach without solving directly the differential equation (equation of motion). The input of impulse is expressed by the instantaneous change of velocity of the structural mass.

In the earthquake-resistant design, the resonance is a key word and it has been investigated extensively. While the resonant equivalent frequency has to be computed for a specified input level by changing the excitation frequency in a parametric manner in dealing with the sinusoidal input (Caughey, 1960a,b; Roberts and Spanos, 1990; Liu, 2000), no iteration is required in the proposed method for the double impulse. This is because the resonant equivalent frequency can be obtained directly without the repetitive procedure. In the double impulse, the analysis can be done without the input frequency (timing of impulses) before the second impulse is input. The resonance can be proved by using energy investigation and the timing of the second impulse can be characterized as the time with zero restoring force. The maximum elastic–plastic response after impulse can be obtained by equating the initial kinetic energy computed by the initial velocity to the sum of hysteretic and elastic strain energies. It should be pointed out that only critical response (upper bound) is captured by the proposed method and the critical resonant

frequency can be obtained automatically for the increasing input level of the double impulse.

In the history of seismic-resistant design of building structures, the earthquake input energy has played an important role together with deformation and acceleration [for example, Housner (1959, 1975), Berg and Thomaides (1960), Housner and Jennings (1975), Zahrah and Hall (1984), Akiyama (1985), and Leger and Dussault (1992)]. While deformation and acceleration can predict and evaluate the performance of a building structure mainly for serviceability, the energy can evaluate the performance of a building structure mainly for safety. Especially energy is appropriate for describing the performance of building structures of different sizes in a unified manner because energy is a global index different from deformation and acceleration as local indices. In fact, in Japan, there are three criteria in parallel (force, deformation, and energy). In 1981, force was introduced as a criterion for safety and in 2000 deformation was introduced as a criterion for safety. More recently in 2005, input energy evaluated from the design velocity response spectrum was used as a criterion. These three criteria are used now in parallel (Building Standard Law in Japan, 1981, 2000, 2005).

A theory of earthquake input energy to building structures under single impulse was shown to be useful for disclosing the property of the energy transfer function (Takewaki, 2004, 2007). This property means that the area of the energy transfer function is constant. The property of the energy transfer function similar to the case of a simple single-degree-of-freedom (SDOF) model has also been clarified for a swaying-rocking model. By using this property, the mechanism of earthquake input energy to the swaying-rocking model including the soil amplification has been made clear under the input of single impulse (Kojima et al., 2015b). However, single impulse may be unrealistic because the frequency characteristic of input cannot be expressed by this input. In order to resolve such issue, the double impulse is introduced in this paper. Furthermore, because the elastic–plastic response is treated, the time-domain formulation is introduced in this paper.

Double Impulse Input

It is well accepted that the fling-step input (fault-parallel) of the near-fault ground motion can be represented by a one-cycle sinusoidal wave and the forward-directivity input (fault-normal) of the near-fault ground motion can be expressed by a series of three sinusoidal wavelets (see **Figure 1**). In this paper and a subsequent paper, it is intended to simplify these typical near-fault ground motions by a double impulse (Kojima et al., 2015a) and a triple impulse. This is because the double impulse and triple impulse have a simple characteristic and a straightforward expression of the response can be expected even for elastic–plastic responses based on an energy approach to free vibrations. Furthermore, the double impulse and triple impulse enable us to describe directly the critical timing of impulses (resonant frequency) which is not easy for the sinusoidal and other inputs without a repetitive procedure.
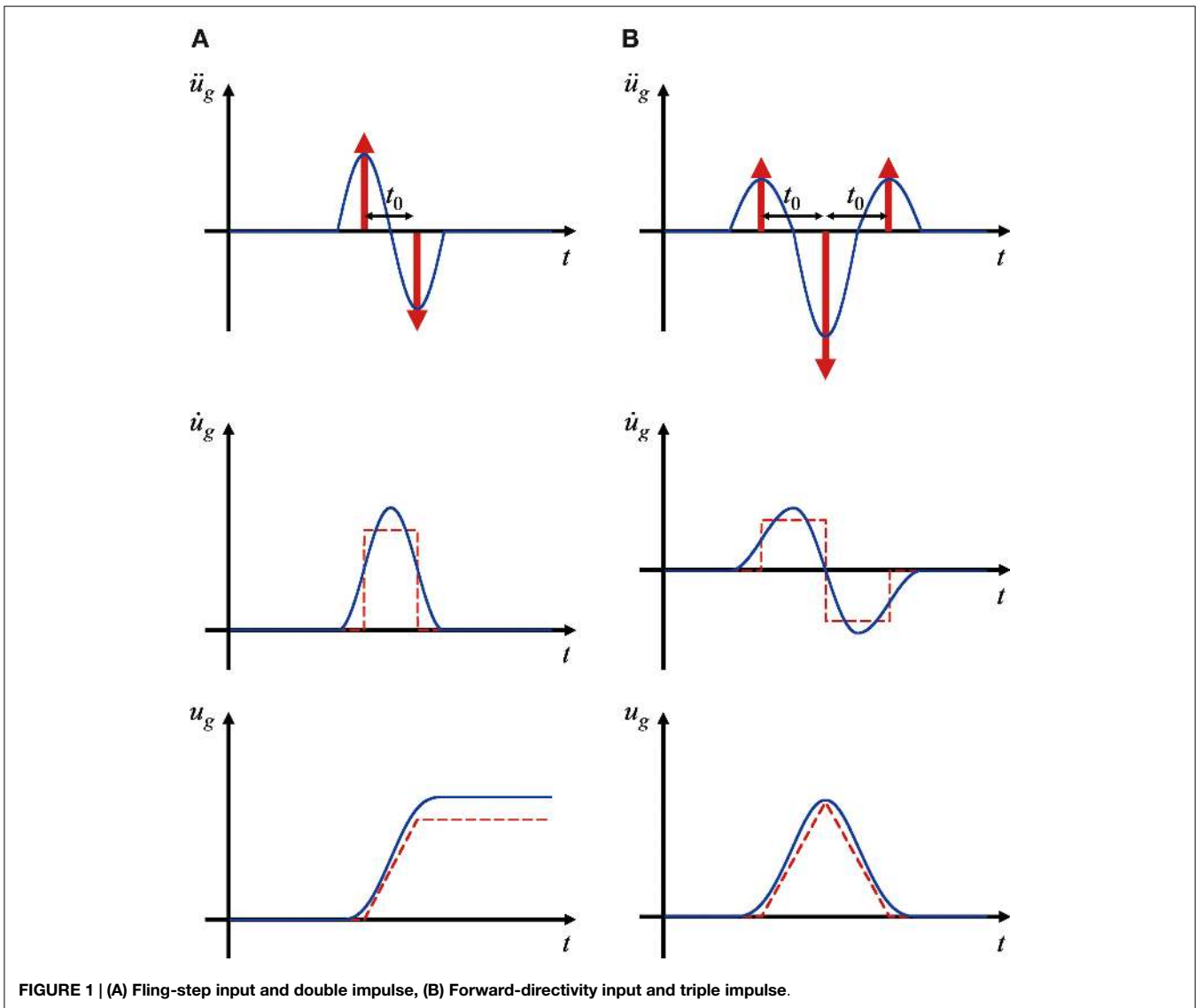
FIGURE 1 | (A) Fling-step input and double impulse, (B) Forward-directivity input and triple impulse.

Consider a ground acceleration $\ddot{u}_g(t)$ as double impulse, as shown in **Figure 1A**, expressed by

$$\ddot{u}_g(t) = V\delta(t) - V\delta(t - t_0) \qquad (1)$$

where V is the given initial velocity and t_0 is the time interval between two impulses. The comparison with the corresponding one-cycle sinusoidal wave as a representative of the fling-step input of the near-fault ground motion (Mavroeidis and Papageorgiou, 2003; Kalkan and Kunnath, 2006) is plotted in **Figure 1A**. The corresponding velocity and displacement of such double impulse and sinusoidal wave are also plotted in **Figure 1A**. It can be understood that the double impulse is a good approximation of the corresponding sinusoidal wave even in the form of velocity and displacement. However, the correspondence in the response should be discussed carefully. This will be conducted in Section "Accuracy Check by Time-history Response Analysis Subjected to the Corresponding One-cycle Sinusoidal Input." The

Fourier transform of $\ddot{u}_g(t)$ of the double impulse input can be derived as

$$
\begin{aligned}
\ddot{U}_g(\omega) &= \int_{-\infty}^{\infty} \left\{ V\delta(t) - V\delta(t - t_0) \right\} e^{-i\omega t} dt \\
&= \int_{-\infty}^{\infty} \left\{ V\delta(t)e^{-i\omega t} - V\delta(t - t_0)e^{-i\omega t_0}e^{-i\omega(t - t_0)} \right\} dt \\
&= V(1 - e^{-i\omega t_0})
\end{aligned}
\qquad (2)
$$

SDOF System

Consider an undamped elastic-perfectly plastic SDOF system of mass m and stiffness k. The yield deformation and yield force are denoted by d_y and f_y (see **Figure 2**). Let $\omega_1 = \sqrt{k/m}$, u, and f denote the undamped natural circular frequency, the displacement of the mass relative to the ground and the restoring force of the model, respectively. The time derivative is denoted by

京都大学
KYOTO UNIVERSITY

A Self-archived copy in
Kyoto University Research Information Repository
https://repository.kulib.kyoto-u.ac.jp

京都大学学術情報リポジトリ
KURENAI 紅
Kyoto University Research Information Repository

Kojima and Takewaki
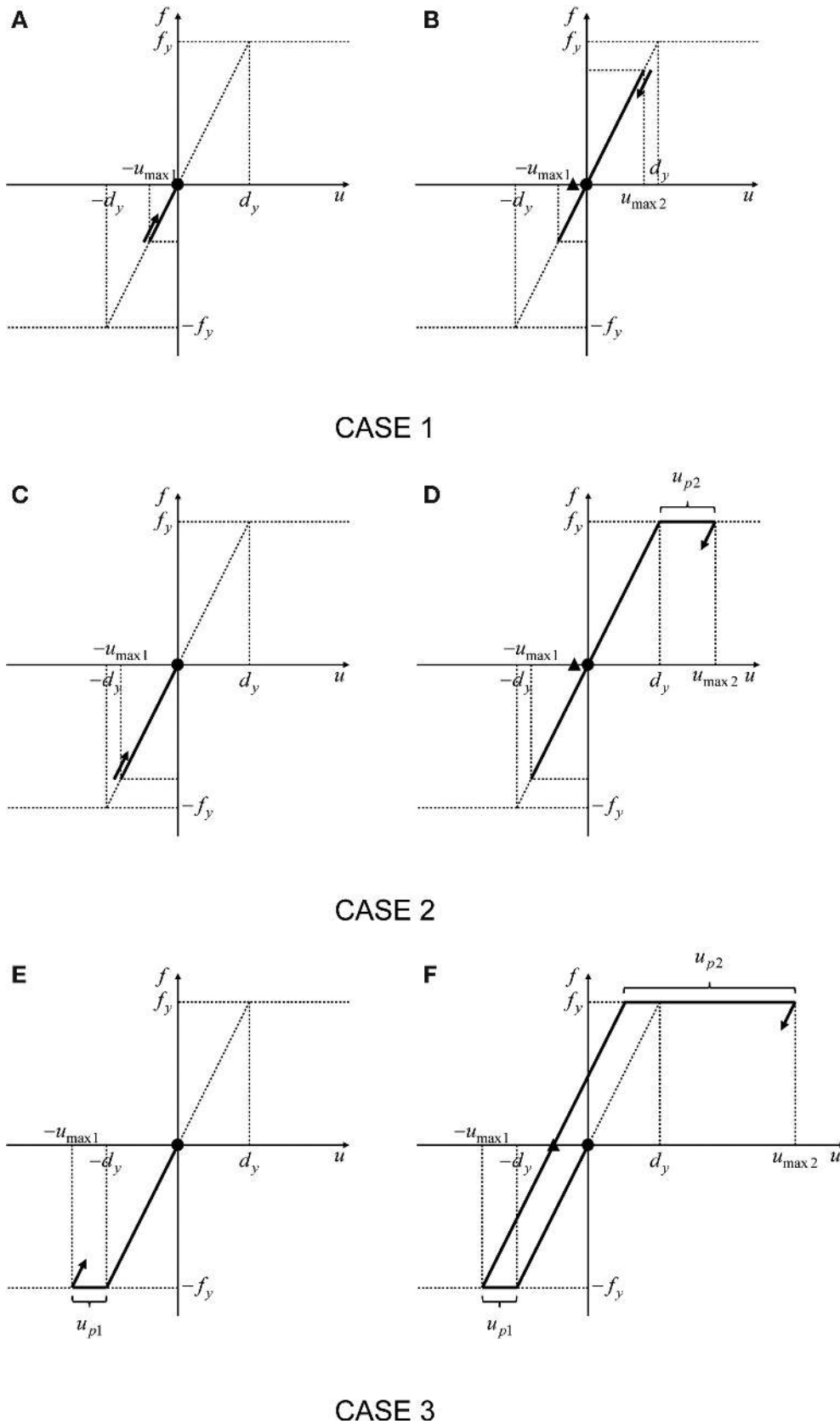
Elastic–plastic near-fault response

FIGURE 2 | Prediction of maximum elastic–plastic deformation under double impulse based on energy approach: (A,B) Case 1: Elastic response; (C,D) Case 2: Plastic response after the second impulse; (E,F) Case 3: Plastic response after the first impulse (●: first impulse, ▲: second impulse).

京都大学
KYOTO UNIVERSITY

A Self-archived copy in
Kyoto University Research Information Repository
https://repository.kulib.kyoto-u.ac.jp

京都大学学術情報リポジトリ
KURENAI 紅
Kyoto University Research Information Repository

Kojima and Takewaki

Elastic–plastic near-fault response

an over-dot. In Section "Maximum Elastic–plastic Deformation of SDOF System Subjected to Double Impulse," these parameters will be dealt with in a non-dimensional or normalized form to derive the relation of permanent interest between the input and the elastic–plastic response. However numerical parameters will be introduced partially in Section "Accuracy Check by Time-history Response Analysis Subjected to the Corresponding One-cycle Sinusoidal Input" to demonstrate an example of actual parameters.

Maximum Elastic–Plastic Deformation of SDOF System Subjected to Double Impulse

The elastic–plastic response to the double impulse can be described by the continuation of free-vibrations. The maximum deformation after the first impulse is denoted by $u_{\max 1}$ and that after the second impulse is expressed by $u_{\max 2}$ as shown in **Figure 2**. The input of each impulse is expressed by the instantaneous change of velocity of the structural mass. Such response can be derived by an energy approach without solving directly the differential equation (equation of motion). The kinetic energy given at the initial stage (the time of the first impulse) and at the time of the second impulse is transformed into the sum of the hysteretic energy and the strain energy corresponding to the yield deformation. By using this rule, the maximum deformation can be obtained in a simple manner.

It should be emphasized that, while the resonant equivalent frequency has to be computed for a specified input level by changing the excitation frequency in a parametric manner in dealing with the sinusoidal input (Caughey, 1960a,b; Roberts and Spanos, 1990; Liu, 2000; Moustafa et al., 2010), no iteration is required in the proposed method for the double impulse. This is because the resonant equivalent frequency (resonance can be proved by using energy investigation: see Appendix) can be obtained directly without the repetitive procedure. As a result, the timing of the second impulse can be characterized as the time with zero restoring force.

Only critical response (upper bound) is captured by the proposed method and the critical resonant frequency can be obtained automatically for the increasing input level of the double impulse. One of the original points in this paper is the introduction of the concept of "critical excitation" in the elastic–plastic response (Drenick, 1970; Abbas and Manohar, 2002; Takewaki, 2007; Moustafa et al., 2010). Once the frequency and amplitude of the critical double impulse are computed, the corresponding one-cycle sinusoidal motion as a representative of the fling-step motion can be identified.

Let us explain the evaluation method of $u_{\max 1}$ and $u_{\max 1}$. The plastic deformation after the first impulse is expressed by u_{p1} and that after the second impulse is denoted by u_{p2}. There are three cases to be considered depending on the yielding stage. Let V_y ($=\omega_1 d_y$) denote the input level of velocity of the double impulse at which the SDOF system just attains the yield deformation after the first impulse.

Figures 2A,B show the maximum deformation after the first impulse and that after the second impulse, respectively, for the

elastic case (Case 1) during the whole stage. $u_{\max 1}$ can be obtained from the following energy conservation law.

$$mV^2/2 = ku_{\max 1}^2/2 \qquad (3)$$

On the other hand, $u_{\max 2}$ can be computed from another energy conservation law.

$$m(2V)^2/2 = ku_{\max 2}^2/2 \qquad (4)$$

As explained in the previous part of this section, the critical timing of the second impulse is the time of zero restoring force and the velocity $-V$ by the second impulse is added to the velocity $-V$ induced by the first impulse (full recovery at the zero restoring force due to zero damping).

Consider next the case (Case 2) where the model goes into the yielding stage after the second impulse. **Figures 2C,D** show the schematic diagram of the response in this case. As in Case 1, $u_{\max 1}$ can be obtained from the energy conservation law.

$$mV^2/2 = ku_{\max 1}^2/2 \qquad (5)$$

On the other hand, $u_{\max 2}$ can be computed from another energy conservation law by regarding the system as a non-linear elastic system tentatively.

$$m(2V)^2/2 = f_y d_y/2 + f_y u_{p2} = f_y d_y/2 + f_y(u_{\max 2} - d_y) \qquad (6)$$

As in the above case, the velocity $-V$ by the second impulse is added to the velocity $-V$ induced by the first impulse.

Consider finally the case (Case 3) where the model goes into the yielding stage even after the first impulse. **Figures 2E,F** show the schematic diagram of the response in this case. $u_{\max 1}$ can be obtained from the following energy conservation law.

$$mV^2/2 = f_y d_y/2 + f_y u_{p1} = f_y d_y/2 + f_y(u_{\max 1} - d_y) \qquad (7)$$

On the other hand, $u_{\max 2}$ can be computed from another energy conservation law.

$$m(v_c + V)^2/2 = f_y d_y/2 + f_y u_{p2} \qquad (8)$$

where v_c is characterized by $mv_c^2/2 = f_y d_y/2$ and u_{p2} is characterized by $u_{\max 2} + (u_{\max 1} - d_y) = d_y + u_{p2}$. In other words, $u_{\max 2}$ can be obtained from

$$m(v_c + V)^2/2 = f_y d_y/2 + f_y(u_{\max 1} + u_{\max 2} - 2d_y). \qquad (9)$$

As in the above case, the velocity $-V$ by the second impulse is added to the velocity $-v_c$ induced by the first impulse (the maximum velocity during the unloading stage).

Figure 3 shows the plot of $u_{\max}/d_y = \max(u_{\max 1}/d_y, u_{\max 2}/d_y)$ with respect to the input level. There are three regions corresponding to Cases 1–3. In Cases 1 and 2, $u_{\max 2}/d_y$ is larger than
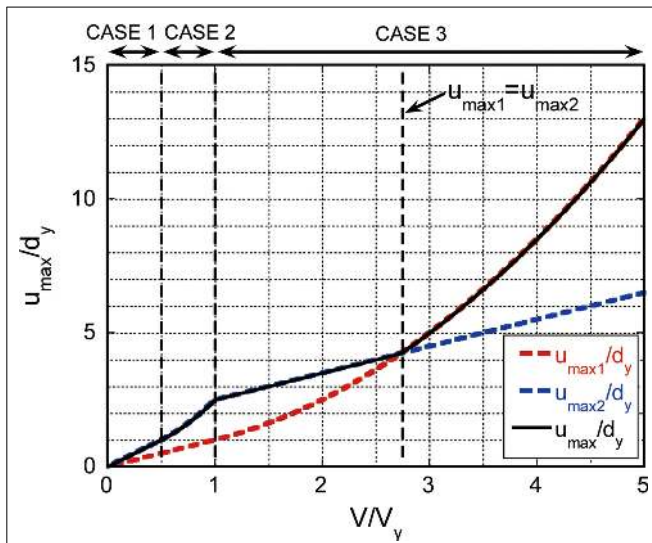
京都大学
KYOTO UNIVERSITY

A Self-archived copy in
Kyoto University Research Information Repository
https://repository.kulib.kyoto-u.ac.jp

京都大学学術情報リポジトリ
KURENAI 紅
Kyoto University Research Information Repository

Kojima and Takewaki

Elastic–plastic near-fault response

FIGURE 3 | Maximum normalized elastic–plastic deformation under double impulse with respect to input level.
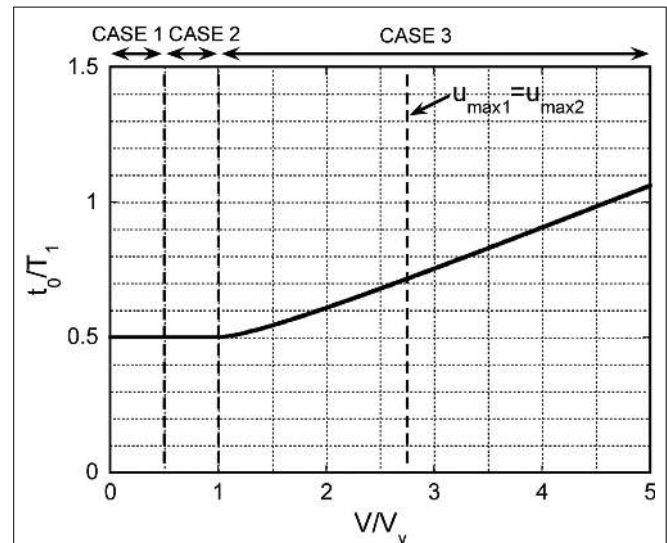

FIGURE 4 | Interval time between the first and second impulses with respect to input level.

$u_{\text{max }1}/d_y$. On the other hand, in Case 3, two regions exist for the boundary case of $u_{\text{max }1} = u_{\text{max }2}$. While $u_{\text{max }2}/d_y$ is larger than $u_{\text{max }1}/d_y$ in the smaller input level, $u_{\text{max }1}/d_y$ is larger than $u_{\text{max }2}/d_y$ in the larger input level.

Figure 4 presents the normalized timing t_0/T_1 ($T_1 = 2\pi/\omega$) of the second impulse with respect to the input level. As stated before, this timing coincides with the time of zero restoring force after the first unloading (see **Figure 2**). It can be observed that the timing is delayed due to plastic deformation as the input level increases. It seems noteworthy to state again that only critical response giving the maximum value of $u_{\text{max }2}/d_y$ is sought by the proposed method and the critical resonant frequency is obtained automatically for the increasing input level of the double impulse. One of the original points in this paper is the tracking of the critical elastic–plastic response.

Accuracy Check by Time-History Response Analysis Subjected to the Corresponding One-Cycle Sinusoidal Input

In order to investigate the accuracy of using the double impulse as a substitute of the corresponding one-cycle sinusoidal wave (representative of the fling-step input), the time-history response analysis of the elastic–plastic SDOF model under the one-cycle sinusoidal wave has been conducted.

In the evaluation procedure, it is important to adjust the input level of the double impulse and the corresponding one-cycle sinusoidal wave based on the equivalence of the Fourier amplitude. **Figure 5** shows one example for the input level $V/V_y = 3$. **Figures 6A,B** illustrate the comparison of the ground displacement and velocity between the double impulse and the corresponding one-cycle sinusoidal wave for the input level $V/V_y = 3$. In **Figure 5** and **Figures 6A,B**, $\omega_1 = 2\pi$(rad/s) ($T_1 = 1.0$ s) and $d_y = 0.16$(m) are used.
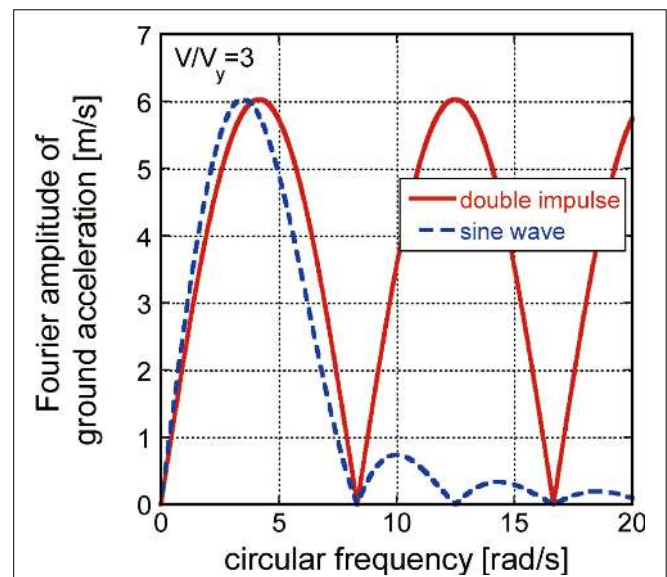

FIGURE 5 | Adjustment of input level of double impulse and the corresponding one-cycle sinusoidal wave based on Fourier amplitude equivalence.

Figure 7 presents the comparison of the ductility (maximum normalized deformation) of the elastic–plastic structure under the double impulse and the corresponding one-cycle sinusoidal wave with respect to the input level. It can be seen that the double impulse provides a fairly good substitute of the one-cycle sinusoidal wave in the evaluation of the maximum deformation if the maximum Fourier amplitude is adjusted appropriately. Although some discrepancy is observed in the large deformation range, that response range is out of interest in the earthquake structural engineering. If desired, other adjustment criterion on input level can be introduced. This is a future issue.
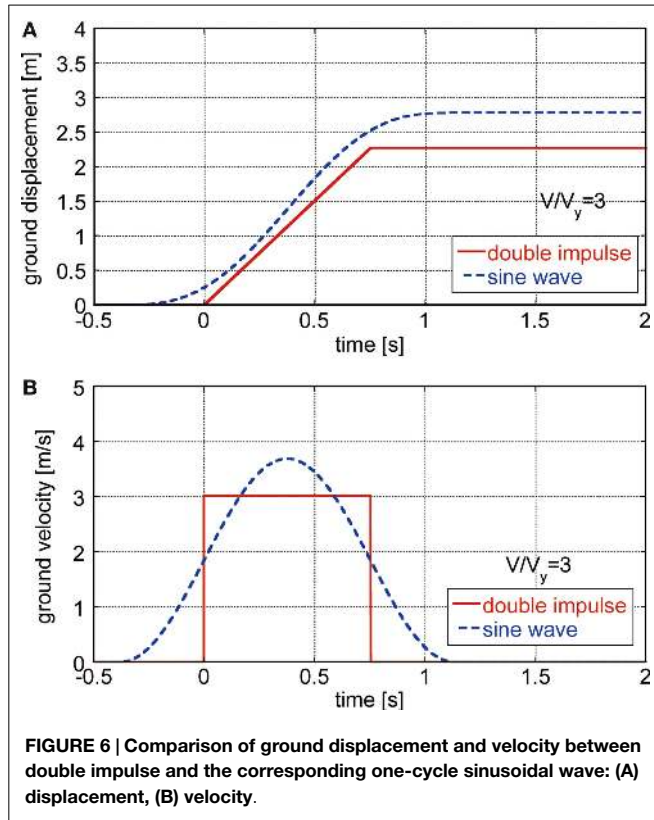
FIGURE 6 | Comparison of ground displacement and velocity between double impulse and the corresponding one-cycle sinusoidal wave: (A) displacement, (B) velocity.
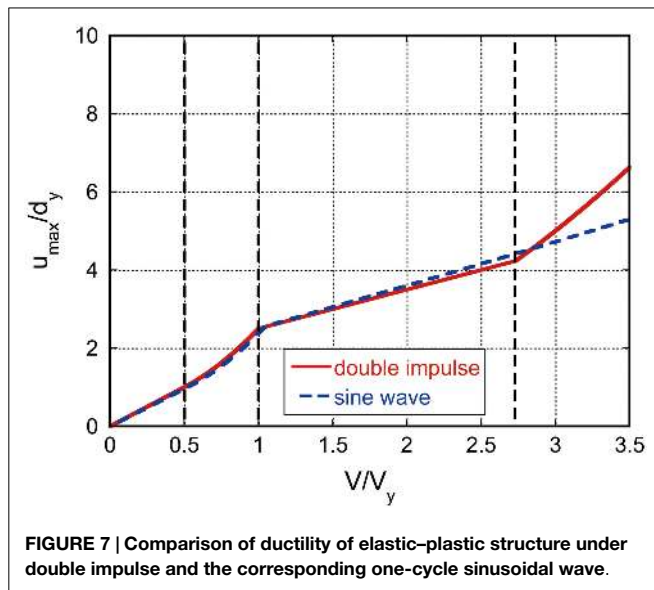

FIGURE 7 | Comparison of ductility of elastic–plastic structure under double impulse and the corresponding one-cycle sinusoidal wave.
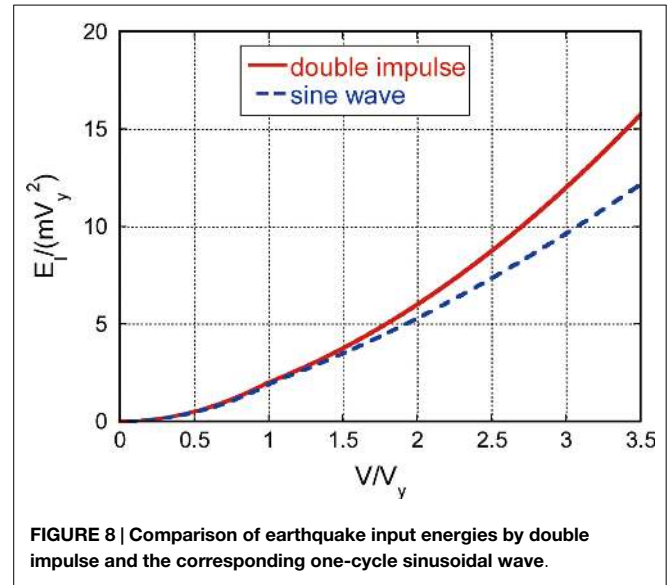

FIGURE 8 | Comparison of earthquake input energies by double impulse and the corresponding one-cycle sinusoidal wave.
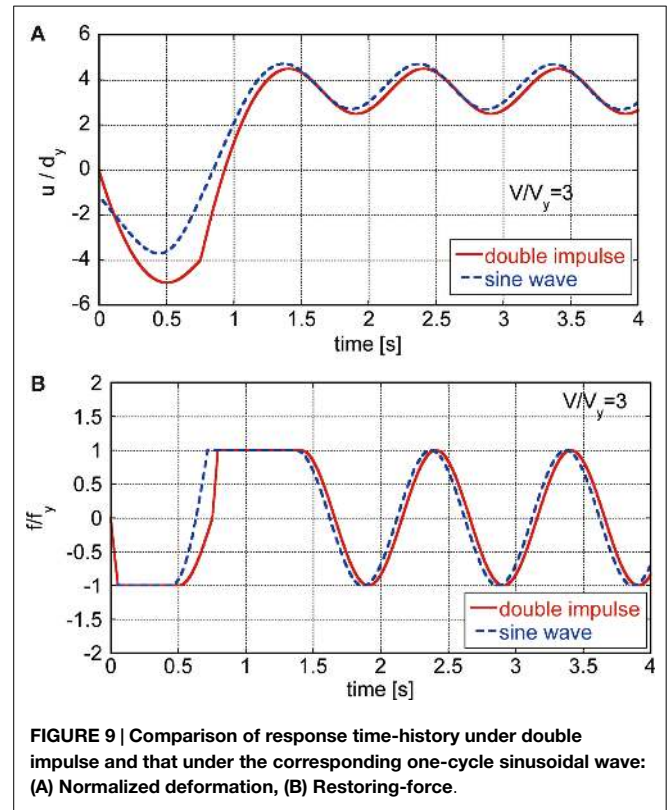

FIGURE 9 | Comparison of response time-history under double impulse and that under the corresponding one-cycle sinusoidal wave: (A) Normalized deformation, (B) Restoring-force.

Figure 8 shows the comparison of the earthquake input energies by the double impulse and the corresponding one-cycle sinusoidal wave. Although a good correspondence can be observed in a lower input level, the double impulse tends to provide a slightly larger upper bound in the larger input level. This property can be understood from the time-history responses shown in **Figures 9** and **10**, i.e., a rather clear difference in deformation after the first impulse.

Figure 9 illustrates the comparison of response time histories (normalized deformation and restoring-force) under the double impulse and those under the corresponding one-cycle sinusoidal wave. The parameters $\omega_1 = 2\pi$ (rad/s) ($T_1 = 1.0$ s), $d_y = 0.16$(m) were also used here. While a rather good correspondence can be seen in the restoring-force, the maximum deformation after the first impulse exhibits a rather larger value in the double impulse. The difference in the initial condition may affect these

response discrepancies. However, it is noteworthy that the maximum deformation after the second impulse demonstrates a rather good correspondence. This may be related to the fact that the effect of the initial condition becomes smaller in this stage. **Figure 10** presents the comparison of the restoring-force characteristic under the double impulse and that under the corresponding one-cycle sinusoidal wave. The parameters $\omega_1 = 2\pi$ (rad/s) ($T_1 = 1.0$ s), $d_y = 0.16$(m) are also used here. As seen in **Figure 9**, while the maximum deformation after the first impulse exhibits a rather larger value in the double impulse compared to that of the corresponding one-cycle sinusoidal wave, the maximum deformation after the second impulse demonstrates a rather good correspondence.
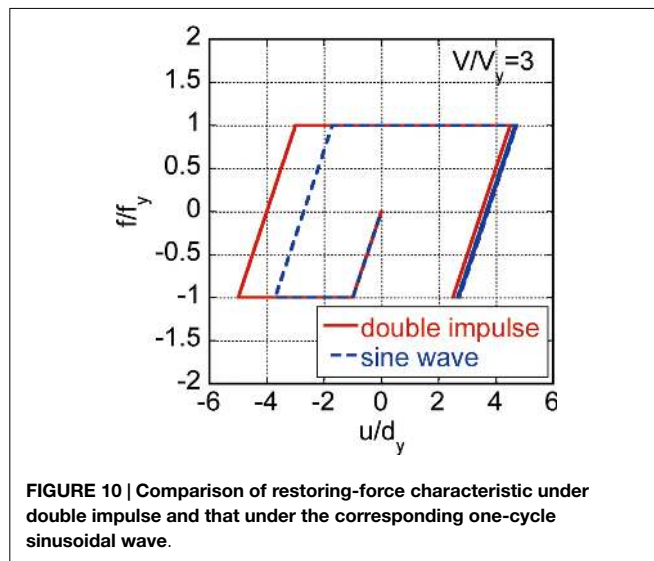

FIGURE 10 | Comparison of restoring-force characteristic under double impulse and that under the corresponding one-cycle sinusoidal wave.

Design of Stiffness and Strength for Specified Velocity and Period of Near-Fault Ground Motion Input and Response Ductility

It is useful to present a flowchart for design of stiffness and strength for the specified velocity and period of the near-fault ground motion input and response ductility. This design concept is based on the philosophy that, if we focus on the worst case of resonance, the safety for other non-resonant cases is guaranteed [see Takewaki (2002)].

Since **Figures 3** and **4** are non-dimensional ones, they can be used for such design. **Figure 11** shows the flowchart for design of stiffness and strength. One example can be drawn as follows:

[*Specified conditions*]: $V = 2$(m/s) (velocity of double impulse), $t_0 = 0.5$(s) (interval of the double impulse and half the period of the corresponding sine wave), $u_{\max}/d_y = 4.0$ (ductility), $m = 4.0 \times 10^6$(kg).

[*Design results*]: $V/V_y = 2.5$, $V_y = 0.80$(m/s), $T_1 = 0.74$(s), $d_y = 0.094$(m), $k = 2.9 \times 10^8$(N/m), $f_y = 2.7 \times 10^7$(N).

From **Figure 3**, $V/V_y = 2.5$ can be obtained for the specified ductility $u_{\max}/d_y = 4.0$. Then $V_y = 0.80$(m/s) is derived from the specified condition $V = 2$(m/s) and $V/V_y = 2.5$. In the next step, $T_1 = 0.74$(s) is found from **Figure 4** for $V/V_y = 2.5$ and $t_0 = 0.5$(s). In this model, $d_y = 0.094$(m) is determined from $V_y = \omega_1 d_y$ and $T_1 (= 2\pi/\omega_1) = 0.74$(s). Finally $k = 2.9 \times 10^8$(N/m) is obtained from $k = \omega_1^2 m$ and $f_y = 2.7 \times 10^7$(N) is derived by $f_y = kd_y$.

It should be reminded that, while most of the previous researches on near-fault ground motions are aimed at disclosing the response characteristics of elastic or elastic–plastic structures with arbitrary stiffness and strength parameters and require tremendous amount of numerical task, the present paper focused
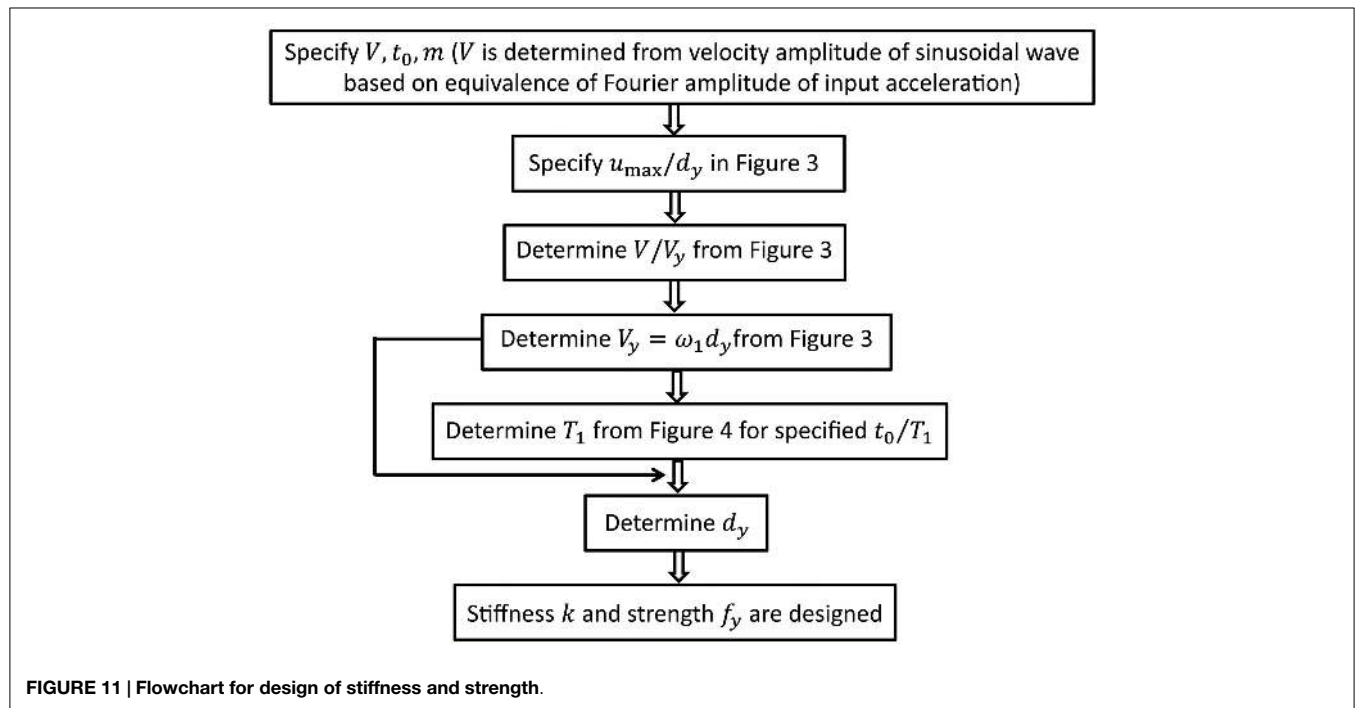

FIGURE 11 | Flowchart for design of stiffness and strength.

京都大学
KYOTO UNIVERSITY

A Self-archived copy in
Kyoto University Research Information Repository
https://repository.kulib.kyoto-u.ac.jp

京都大学学術情報リポジトリ
KURENAI 紅
Kyoto University Research Information Repository

Kojima and Takewaki

Elastic–plastic near-fault response

on the critical response (resonant response) and enabled the drastic reduction of computational works.

Conclusion

The conclusions may be summarized as follows:

(1) The double impulse input has been introduced as a substitute of the fling-step near-fault ground motion and a closed-form solution of the elastic–plastic response of a structure by the critical double impulse input has been derived.

(2) It has been shown that, since only the free-vibration appears in such double impulse input, the energy approach plays an important role in the derivation of the closed-form solution of a complicated elastic–plastic response. In other words the energy approach enables the derivation of the maximum elastic–plastic seismic response without solving the differential equation (equation of motion). In this process, the input of impulse is expressed by the instantaneous change of velocity of the structural mass. The maximum elastic–plastic response after impulse can be obtained by equating the initial kinetic energy computed by the initial velocity to the sum of hysteretic and elastic strain energies. It has been shown that the maximum inelastic deformation can occur either after the first impulse or after the second impulse depending on the input level.

(3) The validity and accuracy of the proposed theory have been investigated through the comparison with the response analysis result to the corresponding one-cycle sinusoidal input as a representative of the fling-step near-fault ground motion. It has been made clear that, if the level of the double impulse is adjusted so as for its maximum Fourier amplitude to coincide with that of the corresponding one-cycle sinusoidal wave, the maximum elastic–plastic deformation to the double impulse exhibits a good correspondence with that to the one-cycle sinusoidal wave.

(4) While the resonant equivalent frequency has to be computed for a specified input level by changing the excitation frequency in a parametric manner in dealing with the sinusoidal input, no iteration is required in the proposed method for the double impulse. This is because the resonant equivalent frequency can be obtained directly without the repetitive procedure. The resonance has been proved by using energy investigation and it has been made clear that the timing of the second impulse can be characterized as the time with zero restoring force.

(5) Only critical response (upper bound) has been captured by the proposed method and it has been shown that the critical resonant frequency can be obtained automatically for the increasing input level of the double impulse. Once the frequency and amplitude of the critical double impulse are computed, the corresponding one-cycle sinusoidal motion as a representative of the fling-step motion can be identified.

(6) A flowchart for design of stiffness and strength for the specified velocity and period of the near-fault ground motion input and response ductility has been proposed using the newly derived non-dimensional relations among response ductility, input velocity, and input period. It has been demonstrated that this flowchart can provide a useful result for such design. Since the critical input of double impulse means the resonant case, the proposed method may be conservative when applied to flexible structures that do not fall in the resonant region.

Acknowledgments

References

Abbas, A. M., and Manohar, C. S. (2002). Investigations into critical earthquake load models within deterministic and probabilistic frameworks. *Earthq. Eng. Struct. Dyn.* 31, 813–832. doi:10.1002/eqe.124.abs

Akiyama, H. (1985). *Earthquake Resistant Limit-State Design for Buildings*. Tokyo: University of Tokyo Press.

Alavi, B., and Krawinkler, H. (2004). Behaviour of moment resisting frame structures subjected to near-fault ground motions. *Earthq. Eng. Struct. Dyn.* 33, 687–706. doi:10.1002/eqe.370

Berg, G. V., and Thomaides, T. T. (1960). "Energy consumption by structures in strong-motion earthquakes," in *Proceedings of 2nd World Conference on Earthquake Engineering*, (Kyoto), 681–696.

Bertero, V. V., Mahin, S. A., and Herrera, R. A. (1978). Aseismic design implications of near-fault San Fernando earthquake records. *Earthq. Eng. Struct. Dyn.* 6, 31–42. doi:10.1002/eqe.4290060105

Bray, J. D., and Rodriguez-Marek, A. (2004). Characterization of forward-directivity ground motions in the near-fault region. *Soil Dyn. Earthq. Eng.* 24, 815–828. doi:10.1016/j.soildyn.2004.05.001

Building Standard Law in Japan. (1981, 2000, 2005). *Earthquake Resistant Design Code*.

Caughey, T. K. (1960a). Sinusoidal excitation of a system with bilinear hysteresis. *J. Appl. Mech.* 27, 640–643. doi:10.1115/1.3644077

Caughey, T. K. (1960b). Random excitation of a system with bilinear hysteresis. *J. Appl. Mech.* 27, 649–652. doi:10.1115/1.3644077

Drenick, R. F. (1970). Model-free design of aseismic structures. *J. Eng. Mech. Div.* 96, 483–493.

Hall, J. F., Heaton, T. H., Halling, M. W., and Wald, D. J. (1995). Near-source ground motion and its effects on flexible buildings. *Earthq Spectra* 11, 569–605. doi:10.1193/1.1585828

Hayden, C. P., Bray, J. D., and Abrahamson, N. A. (2014). Selection of near-fault pulse motions. *J. Geotechnical. Geoenviron. Eng.* 140, 04014030. doi:10.1061/(ASCE)GT.1943-5606.0001129

Housner, G. W. (1959). Behavior of structures during earthquakes. *J. Eng. Mech. Div.* 85, 109–129.

Housner, G. W. (1975). "Measures of severity of earthquake ground shaking," in *Proceedings of the US National Conference on Earthquake Engineering*, (Ann Arbor, MI), 25–33.

Housner, G. W., and Jennings, P. C. (1975). "The capacity of extreme earthquake motions to damage structures," in *Structural and Geotechnical Mechanics*: A Volume Honoring N.M. Newmark, ed. W. J. Hall (Englewood Cliff, NJ: Prentice-Hall), 102–116.

京都大学
KYOTO UNIVERSITY

A Self-archived copy in
Kyoto University Research Information Repository
https://repository.kulib.kyoto-u.ac.jp

京都大学学術情報リポジトリ
KURENAI 紅
Kyoto University Research Information Repository

Kojima and Takewaki

Elastic–plastic near-fault response

Kalkan, E., and Kunnath, S. K. (2006). Effects of fling step and forward directivity on seismic response of buildings. *Earthq. Spectra* 22, 367–390. doi:10.1193/1.2192560

Kalkan, E., and Kunnath, S. K. (2007). Effective cyclic energy as a measure of seismic demand. *J. Earthq. Eng.* 11, 725–751. doi:10.1080/13632460601033827

Khaloo, A. R., Khosravi, H., and Hamidi Jamnani, H. (2015). Nonlinear interstory drift contours for idealized forward directivity pulses using "modified fish-bone" models. *Adv. Struct. Eng.* 18, 603–627. doi:10.1260/1369-4332.18.5.603

Kojima, K., Fujita, K., and Takewaki, I. (2015a). Critical double impulse input and bound of earthquake input energy to building structure. *Front. Built Environ.* 1:5. doi:10.3389/fbuil.2015.00005

Kojima, K., Sakaguchi, K., and Takewaki, I. (2015b). Mechanism and bounding of earthquake energy input to building structure on surface ground subjected to engineering bedrock motion. *Soil Dyn. Earthq. Eng.* 70, 93–103. doi:10.1016/j.soildyn.2014.12.010

Leger, P., and Dussault, S. (1992). Seismic-energy dissipation in MDOF structures. *J. Struct. Eng.* 118, 1251–1269. doi:10.1061/(ASCE)0733-9445(1992)118:5(1251)

Liu, C.-S. (2000). The steady loops of SDOF perfectly elastoplastic structures under sinusoidal loadings. *J. Mar. Sci. Technol.* 8, 50–60.

Mavroeidis, G. P., Dong, G., and Papageorgiou, A. S. (2004). Near-fault ground motions, and the response of elastic and inelastic single-degree-freedom (SDOF) systems. *Earthq. Eng. Struct. Dyn.* 33, 1023–1049. doi:10.1002/eqe.391

Mavroeidis, G. P., and Papageorgiou, A. S. (2003). A mathematical representation of near-fault ground motions. *Bull. Seism. Soc. Am.* 93, 1099–1131. doi:10.1785/0120020100

Moustafa, A., Ueno, K., and Takewaki, I. (2010). Critical earthquake loads for SDOF inelastic structures considering evolution of seismic waves. *Earthq. Struct.* 1, 147–162. doi:10.12989/eas.2010.1.2.147

Mukhopadhyay, S., and Gupta, V. K. (2013a). Directivity pulses in near-fault ground motions – I: identification, extraction and modeling. *Soil Dyn. Earthq. Eng.* 50, 1–15. doi:10.1016/j.soildyn.2013.02.017

Mukhopadhyay, S., and Gupta, V. K. (2013b). Directivity pulses in near-fault ground motions – II: estimation of pulse parameters. *Soil Dyn. Earthq. Eng.* 50, 38–52. doi:10.1016/j.soildyn.2013.02.019

Roberts, J. B., and Spanos, P. D. (1990). *Random Vibration and Statistical Linearization*. New York, NY: Wiley.

Rupakhety, R., and Sigbjörnsson, R. (2011). Can simple pulses adequately represent near-fault ground motions? *J. Earthq. Eng.* 15, 1260–1272. doi:10.1080/13632469.2011.565863

Sasani, M., and Bertero, V. V. (2000). "Importance of severe pulse-type ground motions in performance-based engineering: historical and critical review," in *Proceedings of the Twelfth World Conference on Earthquake Engineering*, (Auckland).

Takewaki, I. (2002). Robust building stiffness design for variable critical excitations. *J. Struct. Eng.* 128, 1565–1574. doi:10.1061/(ASCE)0733-9445(2002)128:12(1565)

Takewaki, I. (2004). Bound of earthquake input energy. *J. Struct. Eng.* 130, 1289–1297. doi:10.1061/(ASCE)0733-9445(2004)130:9(1289)

Takewaki, I. (2007). *Critical Excitation Methods in Earthquake Engineering*, Second Edn. Oxford: Elsevier, 2013.

Takewaki, I., Moustafa, A., and Fujita, K. (2012). *Improving the Earthquake Resilience of Buildings: The Worst Case Approach*. London: Springer.

Takewaki, I., and Tsujimoto, H. (2011). Scaling of design earthquake ground motions for tall buildings based on drift and input energy demands. *Earthq. Struct.* 2, 171–187. doi:10.12989/eas.2011.2.2.171

Vafaei, D., and Eskandari, R. (2015). Seismic response of mega buckling-restrained braces subjected to fling-step and forward-directivity near-fault ground motions. *Struct. Design Tall Spec. Build.* 24, 672–686. doi:10.1002/tal.1205

Xu, Z., Agrawal, A. K., He, W.-L., and Tan, P. (2007). Performance of passive energy dissipation systems during near-field ground motion type pulses. *Eng. Struct.* 29, 224–236. doi:10.1016/j.engstruct.2006.04.020

Yamamoto, K., Fujita, K., and Takewaki, I. (2011). Instantaneous earthquake input energy and sensitivity in base-isolated building. *Struct. Design Tall Spec. Build.* 20, 631–648. doi:10.1002/tal.539

Yang, D., and Zhou, J. (2014). A stochastic model and synthesis for near-fault impulsive ground motions. *Earthq. Eng. Struct. Dyn.* 44, 243–264. doi:10.1002/eqe.2468

Zahrah, T. F., and Hall, W. J. (1984). Earthquake energy absorption in SDOF structures. *J. Struct. Eng.* 110, 1757–1772. doi:10.1061/(ASCE)0733-9445(1984)110:8(1757)

Zhai, C., Chang, Z., Li, S., Chen, Z.-Q., and Xie, L. (2013). Quantitative identification of near-fault pulse-like ground motions based on energy. *Bull. Seism. Soc. Am.* 103, 2591–2603. doi:10.1785/0120120320

Appendix

Proof of Critical Timing of the Second Impulse and Numerical Demonstration

Consider the critical timing of the second impulse. Let v_c denote the velocity of the mass passing the zero restoring-force (zero elastic strain energy) after the first unloading and $v^\star$, $u^\star$ denote the velocity and the elastic deformation component at an arbitrary point between the first unloading and the second yielding. Since the first unloading starts from the state with zero velocity and the elastic strain energy $f_y d_y/2$, the relation $m v_c^2/2 = f_y d_y/2$ holds. From the energy conservation law between the first unloading and the second yielding, the relation $m v^{\star 2}/2 + k u^{\star 2}/2 = f_y d_y/2$ holds. Consider the second impulse at the same time of the state of $v^\star, u^\star$. The total mechanical energy can be expressed by $m(v^\star + V)^2/2 + k u^{\star 2}/2$. Since the relation $m(v^\star + V)^2/2 + k u^{\star 2}/2 = m v^{\star 2}/2 + k u^{\star 2}/2 + m v^\star V + m V^2/2 = f_y d_y/2 + m v^\star V + m V^2/2$ holds and the maximum deformation after the second yielding is caused by the maximum total mechanical energy, the maximum velocity $v^\star$ causes the maximum deformation after the second yielding. This timing is the zero restoring-force after the first unloading. This completes the proof.

In order to confirm the validity of the critical timing shown above, numerical computation has been conducted. Let t_{0c} denote the critical interval between two impulses. **Figure A1** shows the
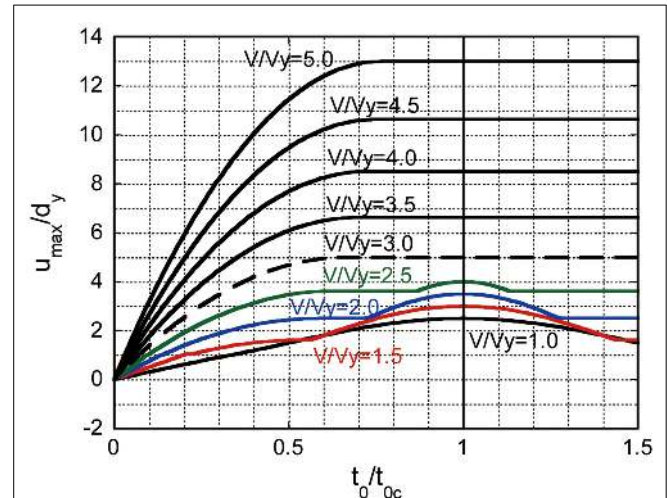

FIGURE A1 | Variation of the maximum deformation under double impulse with respect to the timing of the second impulse.

plot of u_{max}/d_y with respect to t_0/t_{0c}. $t_0/t_{0c} = 1$ indicates the critical timing at zero restoring force. It can be understood that, for larger V/V_y, $t_0/t_{0c} = 1$ is one of the value yielding the maximum value of u_{max}/d_y and, for smaller V/V_y, $t_0/t_{0c} = 1$ certainly gives the maximum value of u_{max}/d_y. This supports the numerical validation of the proof given above.